

## Kaon physics with KLOE

B. SCIASCIA for the KLOE COLLABORATION<sup>(\*)</sup>

*INFN, Laboratori Nazionali di Frascati - Frascati (Rome), Italy*

(ricevuto il 14 Settembre 2010; pubblicato online l'11 Gennaio 2011)

**Summary.** — Kaon physics can test new-physics effects in leptonic or semileptonic decays. A unitarity test of the first row of the CKM mixing matrix is obtained from the precision measurements of  $K_{l3}$  widths for  $K^\pm$ ,  $K_L$ , and (unique to KLOE)  $K_S$ . The KLOE measurement of  $R_K = \Gamma(Ke2)/\Gamma(K\mu2)$  with an accuracy at the % level, aims at finding evidence of deviations from the SM prediction induced by lepton-flavor violation new-physics effects.

PACS 13.20.Eb – Decays of  $K$  mesons.

PACS 12.15.Hh – Determination of Cabibbo-Kobayashi & Maskawa (CKM) matrix elements.

### 1. – Introduction

Purely leptonic and semileptonic decays of  $K$  mesons ( $K \rightarrow \ell\nu$ ,  $K \rightarrow \pi\ell\nu$ ,  $\ell = e, \mu$ ) are mediated in the Standard Model (SM) by tree-level  $W$ -boson exchange. Gauge coupling universality and three-generation quark mixing imply that semileptonic processes such as  $d^i \rightarrow u^j\ell\nu$  are governed by the effective Fermi constant  $G_{ij} = G_\mu V_{ij}$ , where i)  $G_\mu$  is the muon decay constant and ii)  $V_{ij}$  are the elements of the unitary Cabibbo-Kobayashi Maskawa (CKM) matrix. This fact has simple but deep consequences, that go under the name of universality relations. In the SM the effective semileptonic constant  $G_{ij}$  does not depend on the lepton flavor. If one extracts  $V_{ij}$  from different semileptonic transitions assuming quark-lepton gauge universality (*i.e.* normalizing the decay rates with  $G_\mu$ ), the CKM unitarity condition  $\sum_j |V_{ij}|^2 = 1$  should be verified.

<sup>(\*)</sup> F. Ambrosino, A. Antonelli, M. Antonelli, F. Archilli, P. Beltrame, G. Bencivenni, C. Bini, C. Bloise, S. Bocchetta, F. Bossi, P. Branchini, G. Capon, D. Capriotti, T. Capussela, F. Cerasini, P. Ciambone, E. De Lucia, A. De Santis, P. De Simone, G. De Zorzi, A. Denig, A. Di Domenico, C. Di Donato, B. Di Micco, M. Dreucci, G. Felici, S. Fiore, P. Franzini, C. Gatti, P. Gauzzi, S. Giovannella, E. Graziani, M. Jacewicz, V. Kulikov, J. Lee-Franzini, M. Martini, P. Massarotti, S. Meola, S. Miscetti, M. Moulson, S. Müller, F. Murtas, M. Napolitano, F. Nguyen, M. Palutan, A. Passeri, V. Patera, P. Santangelo, B. Sciascia, A. Sibidanov, T. Spadaro, C. Taccini, L. Tortora, P. Valente, G. Venanzoni and R. Versaci.

Beyond the SM, these universality relations can be violated by new contributions to the low-energy  $V-A$  four fermion operators, as well as new non  $V-A$  structures. Therefore, precision tests of the universality relations probe physics beyond the SM and are sensitive to several SM extensions [1-4].

This paper is organized as follows. The present and future status of DAΦNE accelerator and KLOE experiment is briefly reviewed in sect. 2. The world average measurement of  $V_{us}$  is presented in sect. 3 together with the new preliminary KLOE measurements of  $K_L$  and  $K_S$  lifetimes. The KLOE result for  $R_K$  is described in sect. 4.

## 2. – DAΦNE and KLOE: present and future

DAΦNE, the Frascati  $\phi$ -factory, is an  $e^+e^-$  collider working at  $\sqrt{s} \sim m_\phi \sim 1.02$  GeV.  $\phi$  mesons are produced, essentially at rest, with a visible cross section of  $\sim 3.1 \mu\text{b}$ . During year 2008 the Accelerator Division has tested a new interaction scheme with the goal of reaching a peak luminosity of  $5 \times 10^{32} \text{ cm}^{-2} \text{ s}^{-1}$ , a factor of three larger than what previously obtained.

KLOE is a multipurpose detector, mainly consisting of a large cylindrical drift chamber (DC) with an internal radius of 25 cm and an external one of 2 m, surrounded by a lead-scintillating fibers electromagnetic calorimeter (EMC). Both are immersed in the 0.52 T field of a superconducting solenoid. From 2000 to 2006, KLOE has acquired  $2.5 \text{ fb}^{-1}$  of data at the  $\phi(1020)$  peak, plus additional  $250 \text{ pb}^{-1}$  at energies slightly higher or lower than that. A collection of the main physics results of KLOE and details of the detector can be found in ref. [5] and references therein.

For the forthcoming run [6], upgrades have also been proposed for the detector. In a first phase, two different devices will be installed along the beam line to detect the scattered electrons/positrons from  $\gamma\gamma$  interactions. In a second phase, a light-material internal tracker will be installed in the region between the beam pipe and the drift chamber to improve charged vertex reconstruction and to increase the acceptance for low- $p_T$  tracks. Crystal calorimeters will cover the low- $\theta$  region, aiming at increasing acceptance for very forward electrons/photons down to  $8^\circ$ . A new tile calorimeter will be used to instrument the DAΦNE focusing system for the detection of photons coming from  $K_L$  decays in the drift chamber. Implementation of the second phase is planned for late 2011. The integrated luminosity for the two phases should be  $5 \text{ fb}^{-1}$  and  $20 \text{ fb}^{-1}$ , respectively.

## 3. – Measurement of $V_{us}$

Large amount of data has been collected on the semileptonic modes  $K \rightarrow \pi\ell\nu$  by several experiments, BNL-E865, KLOE, KTeV, ISTRA+, and NA48 in the last few years. These data have stimulated a substantial progress on the theoretical inputs, so that most of the theory-dominated errors associated to radiative corrections and hadronic form factors have been reduced below 1%. Presently, the unitarity test

$$(1) \quad |V_{ud}|^2 + |V_{us}|^2 + |V_{ub}|^2 = 1 + \Delta_{\text{CKM}}$$

implies that  $\Delta_{\text{CKM}}$  is consistent with zero at the level of  $6 \times 10^{-4}$ .  $V_{us}$  from  $K \rightarrow \pi\ell\nu$  decays contributes about half of this uncertainty, mostly coming from the hadronic matrix element. Both experimental and theoretical progress in  $K_{\ell 3}$  decays will be needed in order to improve the accuracy on  $\Delta_{\text{CKM}}$  in the future.

TABLE I. – Values of  $|V_{us}|f_+(0)$  extracted from  $K_{l3}$  decay rates.

$K_L e3$	$K_L \mu3$	$K_S e3$	$K^\pm e3$	$K^\pm \mu3$
0.2163(6)	0.2166(6)	0.2155(13)	0.2160(11)	0.2158(14)

It has been shown [4] that presently semileptonic processes and the related universality tests provide constraints on NP that cannot be obtained from other electroweak precision tests and/or direct measurements at the colliders.

In the last years, many efforts have been dedicated to the correct averaging of the rich harvest of recent results in kaon physics. The FLAVIANet kaon working group has published a comprehensive review [7] in 2008 where a detailed description of the averaging procedure can be found. However, the significant progress on both the experimental and theoretical sides, has motivated the same group to publish an updated analysis [8]. Even if these proceedings will focus on the contribution from KLOE, all the  $V_{us}$ -related results presented refer to the FlaviaNet working group outcomes.

After four years of data analysis, KLOE has produced the most comprehensive set of results from a single experiment, measuring the main BRs of  $K_L$ ,  $K^\pm$ , and  $K_S$  (unique to KLOE), including semileptonic and two-body decays; lifetime measurements for  $K_L$  and  $K^\pm$ , form factor slopes from the analysis of  $K_L e3$  and  $K_L \mu3$ . The value of  $|V_{us}|f_+(0)$  has been obtained from KLOE results [10] using the  $K_S$  lifetime from PDG [11] as the only non-KLOE input. The values of  $|V_{us}|f_+(0)$  obtained from the world average of K semileptonic measurements [8] are shown in table I.

The five decay modes agree well within the errors and average to  $|V_{us}|f_+(0) = 0.2163(5)$ , with  $\chi^2/\text{ndf} = 0.77/4$  (Prob = 94%). Significant lepton-universality tests are provided by the comparison of the results from different leptonic channels. Defining the ratio  $r_{\mu e} = |V_{us}|f_+(0)_{\mu3}^2/|V_{us}|f_+(0)_{e3}^2$  we have  $r_{\mu e} = g_\mu^2/g_e^2$ , with  $g_\ell$  the coupling strength at the  $W \rightarrow \ell\nu$  vertex. Lepton universality can be then tested comparing the measured value of  $r_{\mu e}$  with the SM prediction  $r_{\mu e}^{\text{SM}} = 1$ . Averaging charged- and neutral-kaon modes, we obtain  $r_{\mu e} = 1.002(5)$ , to be compared with the results from leptonic pion decays,  $(r_{\mu e})_\pi = 1.0042(33)$  [12], and from leptonic  $\tau$  decays  $(r_{\mu e})_\tau = 1.000(4)$  [13].

Using the determination of  $|V_{us}|f_+(0)$  from  $K_{l3}$  decays and the value  $f_+(0) = 0.959(5)$  (see ref. [8] for a detailed discussion on this choice), we get  $|V_{us}| = 0.2254(13)$ .

Furthermore, a measurement of  $|V_{us}|/|V_{ud}|$  can be obtained from the comparison of the radiation-inclusive decay rates of  $K^\pm \rightarrow \mu^\pm \nu(\gamma)$  and  $\pi^\pm \rightarrow \mu^\pm \nu(\gamma)$ , combined with lattice calculation of  $f_K/f_\pi$  [14]. Using the  $\text{BR}(K^\pm \rightarrow \mu^\pm \nu)$  average value (dominated by KLOE result [15]) and the lattice result  $f_K/f_\pi = 1.193(6)$  (again see ref. [8] for a detailed discussion on this choice), we get  $|V_{us}|/|V_{ud}| = 0.2312(13)$ . This value can be used in a fit together with the measurements of  $|V_{us}|$  from  $K_{l3}$  decays and  $|V_{ud}| = 0.97425(22)$  [16] from superallowed nuclear  $\beta$  decays. The result of this fit is  $|V_{ud}| = 0.97425(22)$  and  $|V_{us}| = 0.2253(9)$ , with  $\chi^2/\text{ndf} = 0.014/1$  (Prob = 91%), from which we get  $1 - (|V_{ud}|^2 + |V_{us}|^2 + |V_{ub}|^2) = -0.0001(6)$  which is in striking agreement with the unitarity hypothesis.

Using these results, we evaluate  $G_{\text{CKM}} = G_\mu \sqrt{|V_{ud}|^2 + |V_{us}|^2 + |V_{ub}|^2} = 1.16633(35) \times 10^{-5} \text{ GeV}^{-2}$ , with  $G_\mu = 1.166371(6) \times 10^{-5} \text{ GeV}^{-2}$ . At present, the sensitivity of the quark-lepton universality test through the  $G_{\text{CKM}}$  measurement is competitive and even better than the measurements from  $\tau$  decays and the electroweak precision tests [17]. Thus unitarity can also be interpreted as a test of the universality of lepton and quark

weak couplings to the  $W$  boson, allowing bounds to be set on extensions of the SM leading to some kind of universality breaking. For instance, the existence of additional  $Z'$  gauge bosons, giving different loop-contributions to muon and semileptonic decays, can break gauge universality [1]. The measurement of  $G_{\text{CKM}}$  can set constraints on the  $Z'$  mass which are competitive with direct search at the colliders. When considering supersymmetric extensions, differences between muon and semileptonic decays can arise in the loop contributions from SUSY particles [2,3]. The slepton-squark mass difference could be investigated improving present accuracy on the unitarity relation by a factor of  $\sim 2-3$ .

**3.1.  $K_L$  lifetime.** – The error on the  $K_L$  lifetime ( $\tau_L$ ) determination is the limiting factor on  $|V_{us}|f_+(0)$  when calculated from  $K_L$ . Using all the available data, KLOE can improve statistical and systematic error over its previous measurements [9,18]. KLOE decided to perform a new  $\tau_L$  measurement based on 46 million  $K_L \rightarrow 3\pi^0$  events, using the same method used in ref. [9].  $K_L$  mesons are tagged by detecting  $K_S \rightarrow \pi^+\pi^-$  decays and the time dependence of the  $K_L \rightarrow 3\pi^0$  decays is used to measure the  $K_L$  lifetime. The  $3\pi^0$  mode is chosen because is the most abundant, has high detection efficiency and the tagging efficiency is almost independent of the  $K_L$  path length. The preliminary result is:  $\tau_L = 50.56 \pm 0.14_{\text{stat}} \pm 0.21_{\text{syst}}$  ns =  $50.56 \pm 0.25$  ns [19] compatible with previous KLOE measurements. The statistical error can be improved by decreasing the lower limit of the fit region, properly accounting for the  $K_L$  beam losses on the regenerating surfaces; the statistical error on the  $K_L$  lifetime is expected to decrease to  $\sim 0.1$  ns. The systematic error arising from the tagging efficiency, due only to detector acceptance, is expected to decrease also.

**3.2.  $K_S$  lifetime.** – KLOE measures the  $K_S$  lifetime ( $\tau_S$ ) with a pure  $K_S$  beam and event-by-event knowledge of the  $K_S$  momentum.  $\tau_S$  can be measured as a function of sidereal time which is interesting for tests of quantum mechanics,  $CPT$  and Lorentz invariance [20]. The lifetime is obtained by fitting the proper time,  $t^*$ , distribution of  $K_S \rightarrow \pi^+\pi^-$  decays. The resolution after event reconstruction is not sufficient for obtaining a lifetime accuracy of 0.1%. The  $t^*$  resolution improves by reconstructing the IP event-by-event using a geometrical fit, selecting events with pions decaying at large angle with respect to the  $K_S$  path, and rejecting poorly measured tracks by a cut on the track fit  $\chi^2$  value. The efficiency of this selection is  $\sim 13\%$ . Since the resolution depends on the  $K_S$  direction, we fit to the proper time distribution from  $-2$  to  $7 \tau_S$  for each of 270 bins in  $\cos(\theta_K)$  and  $\phi_K$ . The statistical error on  $\tau_S$  is less than 0.1%. With the full KLOE statistics the preliminary result  $\tau_S = (89.56 \pm 0.03 \pm 0.07)$  ps [21] has been obtained, with the aim of reaching  $\sim 0.03$  ps final systematic uncertainty. A relative error of 0.03% on  $\tau_S$  is expected scaling this result to the KLOE-2 data sample.

#### 4. – Measurement of $R_K = \Gamma(Ke2)/\Gamma(K\mu2)$

The SM prediction of  $R_K$  benefits from cancellation of hadronic uncertainties to a large extent and therefore can be calculated with high precision. Including radiative corrections, the total uncertainty is less than 0.5 per mil [1,22]:

$$(2) \quad R_K = (2.477 \pm 0.001) \times 10^{-5}.$$

Since the electronic channel is helicity-suppressed by the  $V-A$  structure of the charged weak current,  $R_K$  can receive contributions from physics beyond the SM, for example

from multi-Higgs effects inducing an effective pseudoscalar interaction. It has been shown in ref. [23] that deviations from the SM of up to few percent on  $R_K$  are quite possible in minimal supersymmetric extensions of the SM and in particular should be dominated by lepton-flavor violating contributions with tauonic neutrinos emitted in the electron channel:

$$(3) \quad R_K = R_K^{\text{SM}} \times \left[ 1 + \frac{m_K^4}{m_H^4} \frac{m_\tau^2}{m_e^2} |\Delta_R^{31}|^2 \tan^6 \beta \right],$$

where  $M_H$  is the charged-Higgs mass,  $\Delta_R^{31}$  is the effective  $e - \tau$  coupling constant depending on MSSM parameters, and  $\tan \beta$  is the ratio of the two vacuum expectation values. Note that the pseudoscalar constant  $f_K$  cancels in  $R_K^{\text{SM}}$ . In order to compare with the SM prediction at this level of accuracy, one has to treat carefully the effect of radiative corrections, which contribute to nearly half the  $K_{e2\gamma}$  width. In particular, the SM prediction of eq. (3) is made considering all photons emitted by the process of internal bremsstrahlung (IB) while ignoring any contribution from structure-dependent direct emission (DE). Of course both processes contribute, so in the analysis DE is considered as a background which can be distinguished from the IB width by means of a different photon energy spectrum.

Using the present KLOE dataset collected at the  $\phi$  peak, and corresponding to  $\sim 3.6$  billion  $K^+K^-$  pairs, a measurement of  $R_K$  with an accuracy of about 1% has been performed.  $\phi$  mesons are produced, essentially at rest and decay into  $K^+K^-$  pairs with a BR of  $\sim 49\%$ . Kaons get a momentum of  $\sim 100$  MeV which translates into a low speed,  $\beta_K \sim 0.2$ .  $K^+$  and  $K^-$  decay with a mean length of  $\lambda_\pm \sim 90$  cm and can be distinguished from their decays in flight to one of the two-body final states  $\mu\nu$  or  $\pi\pi^0$ . The kaon pairs from  $\phi$  decay are produced in a pure  $J^{PC} = 1^{--}$  quantum state, so that observation of a  $K^+$  in an event signals, or tags, the presence of a  $K^-$  and vice versa; highly pure and nearly monochromatic  $K^\pm$  beams can thus be obtained and exploited to achieve high precision in the measurement of absolute BRs. KLOE DC constitutes a fiducial volume for  $K^\pm$  decays extending for  $\sim 1\lambda_\pm$ . The momentum resolution for tracks at large polar angle is  $\sigma_p/p \leq 0.4\%$ . The c.m. momenta reconstructed from identification of 1-prong  $K^\pm \rightarrow \mu\nu, \pi\pi^0$  decay vertices in the DC peak around the expected values with a resolution of 1–1.5 MeV, thus allowing clean and efficient  $K^\pm$  tagging. Given the  $K^\pm$  decay length, the selection of one-prong  $K^\pm$  decays in the DC required to tag  $K^\mp$  has an efficiency smaller than 50%. In order to keep the statistical uncertainty on the number of  $K \rightarrow e\nu$  counts below 1%, a “direct search” for  $K \rightarrow e\nu$  and  $K \rightarrow \mu\nu$  decays is performed, without tagging. Since the wanted observable is a ratio of BRs for two channels with similar topology and kinematics, one expects to benefit from some cancellation of the uncertainties on tracking, vertexing, and kinematic identification efficiencies. Small deviations in the efficiency due to the different masses of  $e$ 's and  $\mu$ 's will be evaluated using MC. Selection starts by requiring a kaon track decaying in a DC fiducial volume (FV) with laboratory momentum between 70 and 130 MeV, and a secondary track of relatively high momentum (above 180 MeV). The FV is defined as a cylinder parallel to the beam axis with length of 80 cm, and inner and outer radii of 40 and 150 cm, respectively. Quality cuts are applied to ensure good track fits. A powerful kinematic variable used to distinguish  $K \rightarrow e\nu$  and  $K \rightarrow \mu\nu$  decays from the background is calculated from the track momenta of the kaon and the secondary particle: assuming  $m_\nu = 0$ , the squared mass of the secondary particle ( $m_\ell^2$ ) is evaluated. The selection applied is enough for clean identification of a  $K \rightarrow \mu\nu$  sample, while further rejection

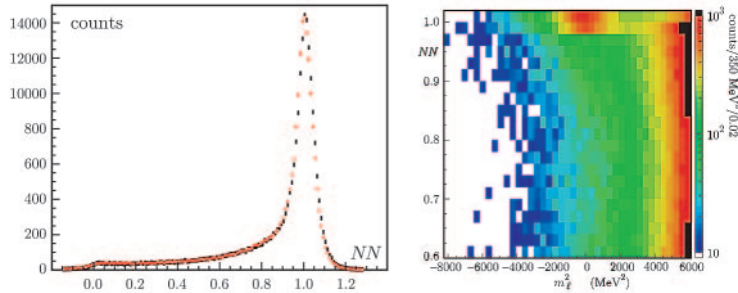


Fig. 1. – (Colour on-line) Left: neural-network output,  $NN$ , for electrons of a  $K_L \rightarrow \pi e \nu$  sample from data (black) and MC (red). Right: data density in the  $(NN, m_e^2)$ -plane: the signal is clearly visible at  $m_e^2 \sim 0$  and  $NN \sim 1$ .

is needed in order to identify  $K \rightarrow e \nu$  events: the background, which is dominated by badly reconstructed  $K \rightarrow \mu \nu$  events, is  $\sim 10$  times more frequent than the signal in the region around  $m_e^2$ .

Information from the EMC is used to improve background rejection. To this purpose, we extrapolate the secondary track to the EMC surface and associate it to a nearby EMC cluster. For electrons, the associated cluster is close to the EMC surface and the cluster energy  $E_{cl}$  is a measurement of the particle momentum  $p_{ext}$ , so that  $E_{cl}/p_{ext}$  peaks around 1. For muons, clusters tend to be more in depth in the EMC and  $E_{cl}/p_{ext}$  tends to be smaller than 1, since only the kinetic energy is visible in the EMC. Electron clusters can also be distinguished from  $\mu$  (or  $\pi$ ) clusters, since electrons shower and deposit their energy mainly in the first plane of EMC, while muons behave like minimum ionizing particles in the first plane and deposit a sizable fraction of their kinetic energy from the third plane onward, when they are slowed down to rest (Braggs peak). Particle identification has been therefore based on the asymmetry of energy deposits between the first and the next-to-first planes, on the spread of energy deposits on each plane, on the position of the plane with the maximum energy, and on the asymmetry of energy deposits between the last and the next-to-last planes. All information is combined with neural network ( $NN$ ) trained on  $K_L \rightarrow \pi l \nu$  data, taking into account variations of the EMC response with momentum and impact angle on the calorimeter. The distribution of the  $NN$  output for an independent  $K_L \rightarrow \pi e \nu$  sample is shown in the left panel of fig. 1 for data and Monte Carlo (MC). Additional separation has been obtained using time-of-flight information. The number of  $K \rightarrow e \nu(\gamma)$  is determined with a binned likelihood fit to the two-dimensional  $NN$  vs.  $m_e^2$  distribution. The data distribution of  $NN$  as a function of  $m_e^2$  is shown in fig. 1 right. A clear  $K \rightarrow e \nu$  signal can be seen at  $m_e^2 \sim 0$  and  $NN \sim 1$ . Distribution shapes for signal and  $K \mu 2$  background, other sources being negligible, are taken from MC; the normalization factors for the two components are the only fit parameters. In the fit region, a small fraction of  $K \rightarrow e \nu(\gamma)$  events is due to the direct-emission structure-dependent component (DE): the value of this contamination,  $f_{DE}$ , is fixed in the fit to the expectation from simulation. This assumption has been evaluated by performing a dedicated measurement of DE, which yielded as a by-product a determination of  $f_{DE}$  with a 4% accuracy [24]. This implies a systematic error on  $Ke2$  counts of 0.2%, as obtained by repeating the fit with values of  $f_{DE}$  varied within its uncertainty. In the fit region, we count  $7064 \pm 102 K^+ \rightarrow e^+ \nu(\gamma)$  and  $6750 \pm 101 K^- \rightarrow e^- \nu(\gamma)$  events.



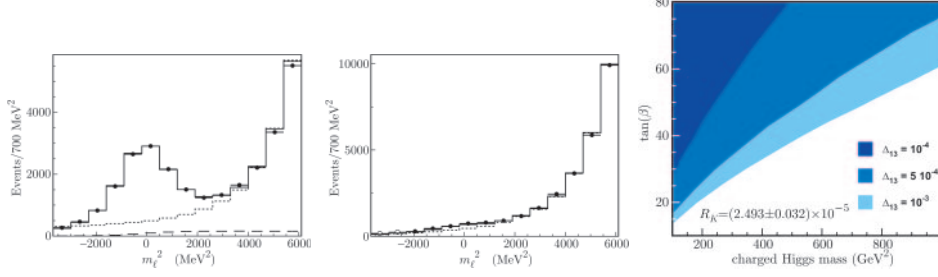


Fig. 2. – Fit projections onto the  $m_\ell^2$  axis for  $NN > 0.98$  (left) and  $NN < 0.98$  (center), for data (black dots), MC fit (solid line), and  $K\mu 2$  background (dotted line). The contribution from  $Ke 2$  events with  $E_\gamma > 10$  MeV is visible in the left panel (dashed line). Right: excluded regions at 95% CL in the plane  $M_H$ - $\tan\beta$  for  $\Delta_R^{31} = 10^{-4}, 5 \times 10^{-3}, 10^{-3}$ .

Figure 2 shows the sum of fit results for  $K^+$  and  $K^-$  projected onto the  $m_\ell^2$  axis in a signal ( $NN > 0.98$ ) and a background ( $NN < 0.98$ ) enhanced region. To assess the uncertainty on the  $R_K$  measurement arising from limited knowledge of the momentum resolution we have examined the agreement between the  $m_\ell^2$  distributions for data and MC in the  $K\mu 2$  region. For the  $NN$  distribution, the EMC response at the cell level has been tuned by comparing data and MC samples. In order to evaluate the systematic error associated with these procedures, we studied the result variation with different fit range values, corresponding to a change for the overall  $Ke 2$  purity from  $\sim 75\%$  to  $\sim 10\%$ . The results are stable within statistical fluctuations. A systematic uncertainty of 0.3% for  $R_K$  is derived *à la* PDG [11] by scaling the uncorrelated errors so that the reduced  $\chi^2$  value of results is 1.

The number of  $K\mu 2$  events in the same data set is extracted from a fit to the  $m_\ell^2$  distribution. The fraction of background events under the muon peak is estimated from MC to be  $< 0.1\%$ . We count  $2.878 \times 10^8 (2.742 \times 10^8) K_\mu^+ 2 (K_\mu^- 2)$  events. Difference in  $K^+$  and  $K^-$  counting is ascribed to  $K^-$  nuclear interactions in the material traversed.

The ratio of  $Ke 2$  to  $K\mu 2$  efficiency is evaluated with MC and corrected for data-to-MC ratios using control samples. To check the corrections applied we also measured  $R_3 = \text{BR}(Ke 3)/\text{BR}(K\mu 3)$ , in the same data sample and by using the same methods for the evaluation of the efficiency as for the  $R_K$  analysis. We found  $R_3 = 1.507(5)$  and  $R_3 = 1.510(6)$ , for  $K^+$  and  $K^-$ , respectively. These are in agreement within a remarkable accuracy with the expectation from world-average [7] form-factor slope measurements,  $R_3 = 1.506(3)$ .

The final result is  $R_K = (2.493 \pm 0.025 \pm 0.019) \times 10^{-5}$  [24]. The 1.1% fractional statistical error has contributions from signal count fluctuation (0.85%) and background subtraction. The 0.8% systematic error has a relevant contribution (0.6%) from the statistics of the control samples used to evaluate corrections to the MC. The result does not depend on  $K$  charge: quoting only the uncorrelated errors,  $R_K(K^+) = 2.496(37)10^{-5}$  and  $R_K(K^-) = 2.490(38)10^{-5}$ . The result in agreement with SM prediction of eq. (2). Including the new KLOE result, the world average reaches an accuracy at the % level:  $R_K = 2.468(25) \times 10^{-5}$ . In the framework of MSSM with LFV couplings, the  $R_K$  value can be used to set constraints in the space of relevant parameters (see eq. (3)). The regions excluded at 95% CL in the plane  $\tan\beta$  charged Higgs mass are shown in the right panel of fig. 2 for different values of the effective LFV coupling  $\Delta_R^{31}$ .

## 5. – Conclusions

The experimental precision in leptonic and semileptonic kaon decays is nicely matched below the percent level by theoretical precision, allowing to perform very precise measurements of SM parameters and to set stringent bounds on physics beyond the SM. KLOE contributed with the most comprehensive set of results from a single experiment, giving a fundamental contribution to the 0.2% world accuracy on the determination of  $|V_{us}|f_+(0)$ . KLOE result on  $R_K$  improves the accuracy with which it is known by a factor of 5 with respect to the present world average and allows severe constraints to be set on new physics contributions in the MSSM with lepton flavor violating couplings.

## REFERENCES

- [1] MARCIANO W. J. and SIRLIN A., *Phys. Rev. D*, **35** (1987) 1672.
- [2] HAGIWARA K., MATSUMOTO S. and YAMADA Y., *Phys. Rev. Lett.*, **75** (1995) 3605, [hep-ph/9507419](#).
- [3] KURYLOV A. and RAMSEY-MUSOLF M. J., *Phys. Rev. Lett.*, **88** (2002) 071804, [hep-ph/0109222](#).
- [4] CIRIGLIANO V., JENKINS J. and GONZALEZ-ALONSO M., *Nucl. Phys. B*, **830** (2010) 95, 0908.1754.
- [5] BOSSI F., DE LUCIA E., LEE-FRANZINI J., MISCETTI S. and PALUTAN M. (KLOE), *Riv. Nuovo Cimento*, **31** (2008) 531, 0811.1929.
- [6] BECK R. *et al.* (KLOE-2), Letter of Intent for the KLOE-2 Roll-in (2007) LNF-07/19(IR).
- [7] ANTONELLI M. *et al.*, FLAVIANet working group on kaon decays (2008) 0801.1817.
- [8] ANTONELLI M. *et al.*, *Eur. Phys. J. C*, **69** (2010) 399.
- [9] AMBROSINO F. *et al.* (KLOE), *Phys. Lett. B*, **626** (2005) 15, [hep-ex/0507088](#).
- [10] AMBROSINO F. *et al.* (KLOE), *JHEP*, **04** (2008) 059, 0802.3009.
- [11] AMSLER C. *et al.* (PARTICLE DATA GROUP), *Phys. Lett. B*, **667** (2008) 1.
- [12] RAMSEY-MUSOLF M. J., SU S. and TULIN S., *Phys. Rev. D*, **76** (2007) 095017, 0705.0028.
- [13] DAVIER M., HOCKER A. and ZHANG Z., *Rev. Mod. Phys.*, **78** (2006) 1043, [hep-ph/0507078](#).
- [14] MARCIANO W. J., *Phys. Rev. Lett.*, **93** (2004) 231803, [hep-ph/0402299](#).
- [15] AMBROSINO F. *et al.* (KLOE), *Phys. Lett. B*, **632** (2006) 76.
- [16] HARDY J. C. and TOWNER I. S., *Phys. Rev. C*, **79** (2009) 055502.
- [17] MARCIANO W. J., *PoS, KAON* (2008) 003.
- [18] AMBROSINO F. *et al.* (KLOE), *Phys. Lett. B*, **632** (2006) 43, [hep-ex/0508027](#).
- [19] BOCCHETTA S. *et al.* (KLOE), *PoS, KAON09* (2009) 006.
- [20] AOKI S. *et al.*, *Astron. Astrophys.*, **105** (1982) 359.
- [21] DREUCCI M. *et al.* (KLOE), *PoS, EPS-HEP09* (2009) 198.
- [22] CIRIGLIANO V. and ROSELL I., *Phys. Rev. Lett.*, **99** (2007) 231801, 0707.3439.
- [23] MASIERO A., PARADISI P. and PETRONZIO R., *Phys. Rev. D*, **74** (2006) 011701, [hep-ph/0511289](#).
- [24] AMBROSINO F. *et al.* (KLOE), *Eur. Phys. J. C*, **64** (2009) 627, 0907.3594.